Journal of Magnetic Resonance 259 (2015) 121–125

Contents lists available at ScienceDirect

Journal of Magnetic Resonance

journal homepage: www.elsevier.com/locate/jmr

Suppression of radiation damping for high precision quantitative NMR

Kevin Bayle, Maxime Julien, Gérald S. Remaud, Serge Akoka *

EBSI team, Interdisciplinary Chemistry: Synthesis, Analysis, Modeling (CEISAM), University of Nantes-CNRS UMR 6230, 2 rue de la Houssinière, BP 92208, F-44322 Nantes cedex 3, France

ARTICLE INFO

Article history:
Received 8 July 2015
Revised 10 August 2015
Available online 19 August 2015

Keywords:
Radiation damping
Quantitative NMR

ABSTRACT

True quantitative analysis of concentrated samples by ^{1}H NMR is made very difficult by Radiation Damping. A novel NMR sequence (inspired by the WET NMR sequence and by Outer Volume Saturation methods) is therefore proposed to suppress this phenomenon by reducing the spatial area and consequently the number of spins contributing to the signal detected. The size of the detected volume can be easily chosen in a large range and line shape distortions are avoided thanks to a uniform signal suppression of the outer volume. Composition of a mixture can as a result be determined with very high accuracy (precision and trueness) at the per mille level whatever the concentrations and without hardware modification.

1. Introduction

Nuclear magnetic resonance (NMR) is a highly versatile spectroscopic technique with applications in a large range of disciplines, from physics and chemistry to biology and medicine. Because NMR is a quantitative technique, and has the recognized advantage of being both non-destructive and non-specific (i.e. all molecular species present can be detected simultaneously), its potential for quantitative analysis is considerable. The application of quantitative NMR has been reported in numerous fields such as pharmaceutical analysis [1] or metabolic studies [2,3]. In the vast majority of studies reported so far, the so-called qNMR [4] methodology is used which exploits a very standardized 1D ^{1}H NMR protocol and concerns diluted samples. However, an accurate quantitative analysis of samples by ^{1}H NMR (i.e. the precise and true determination of the concentrations [5]) is made very difficult on concentrated samples since it is then difficult to avoid signal saturation and, most importantly, the phenomenon of radiation damping. This phenomenon was first described by Suryan [6], even if denomination actually originates from Bloembergen and Pound who described it mathematically [7]. Radiation damping can be described by a self-induced back-action field. The precessing magnetization creates a current in the coil, and the current, in turn, induces a magnetic field that acts back on the sample. This transverse radio-frequency field (which is 90° phase-shifted with respect to the transverse magnetization) depends on the quality factor value, the filling factor of the probe, and the magnetization's amplitude (directly proportional to n: number of resonating spins). The system is then brought back to equilibrium more quickly than by mere relaxation phenomena (for a more detailed description of radiation damping see Ref. [8]). Theoretically, it does not degrade the integral of the resulting transformed peak, as the amplitude of the first point of the FID is unaffected (assuming the transverse relaxation time is large compared to the delay between excitation and detection of the NMR signal). However, it results in deformation/widening of peak shape as well as in a shift of the relative phase of multiplets. Consequently, the accuracy of peak area measurements can be greatly affected. This effect is in most cases very small and can be neglected; however, it appears significant when concentrated samples are analyzed in an intense magnetic field. Furthermore, integration becomes difficult since the baseline is affected over an appreciable frequency range around each intense line.

Several methods have been proposed to control radiation damping [8]. A simple solution is to dilute the sample. When dilution is inconvenient or undesirable, one can also use very small filling factors to the same effect. On the other hand, to work on a concentrated sample in a regular tube, the simplest remedy is to grossly mistune the receiver coil. However, a large portion of the transmitted pulse power is reflected, and pulse durations become very long. Radiation damping effects may be also eliminated from the NMR spectrum either using hardware modifications [9–12] or dedicated pulse sequences [13–16]. All these approaches are fairly

* Corresponding author at: Chimie et Interdisciplinarité: Synthèse, Analyse, Modélisation (CEISAM), UMR 6230, Faculté des Sciences, BP 92208, 2 rue de la Houssinière, F-44322 Nantes Cedex 03, France. Fax: +33 (0)2 51 12 57 12.
E-mail address: serge.akoka@univ-nantes.fr (S. Akoka).

http://dx.doi.org/10.1016/j.jmr.2015.08.007
1090-7807/

successful in eliminating RD to a large extent, but up to now, none of them were found appropriate to achieve highly precise quantification in concentrated samples.

In this paper, a novel NMR sequence (inspired by the WET NMR sequence [17,18] and by Outer Volume Saturation methods [19]) has therefore been designed to determine composition of a given mixture with a high precision (per mille, ‰) whatever the concentrations and without hardware modification. Radiation damping is managed by reducing the spatial area and therefore the number n of spins contributing to the signal detected by the receiver.

2. Method

2.1. Principle

Radiation damping suppression can be obtained by creating a small transverse magnetization while simultaneously eliminating z-magnetization [16]. That is notably done by the NORD sequence [16] which uses a spin echo together with two slightly different gradient pulses during each half of the echo. This method provides good quality proton spectra on concentrated samples. However, with such strategy two issues arise: (i) in the case of small echo times, precision is affected by small line shape distortions triggered by Eddy currents whereas (ii) trueness is deteriorated by T_2 weighting of peak areas in the situation of long echo times.

We have therefore developed a method to obtain the same result in avoiding gradient commutation close to the sampling period. This method can be seen as a merge of the WET sequence [17,18] and methods used in localized spectroscopy to saturate the signal arising from outside the volume of interest [19] (Fig. 1). In the following, we will name this sequence DWET: for Double WET.

The basic segment (between brackets) is constituted of two selective RF pulses applied simultaneously with the gradient g_e and followed by a dephasing gradient pulse g_i. Each selective pulse excites a bandwidth ΔF. The medium frequency of the first one is $+\delta f$ (with $\delta f > \Delta F/2$), and that of the second one is $-\delta f$. If the B_1 field is perfectly homogeneous within the RF coil, one of these basic segments flips all the magnetization in the transverse plan, except for spins resonating (in presence of g_e) at frequencies between $-\delta f + \Delta F/2$ and $+\delta f - \Delta F/2$.

However, the B_1 profile of an RF coil is never rectangular, and when v_1^{max} (maximum amplitude of the selective pulses) is adjusted to induce a $\pi/2$ flip angle in the middle of the sample, this flip angle is however significantly smaller on the edge. Repetition of the basic segment is therefore necessary to improve suppression

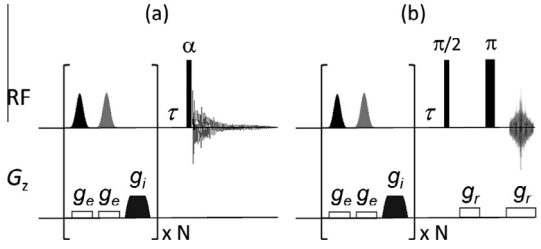

Fig. 1. The DWET sequence (a) and sequence used for adjustments (b). The basic segment (between brackets) is constituted of two selective RF pulses applied simultaneously with the gradient g_e and followed by a dephasing gradient pulse g_i. Each selective pulses excites a bandwidth ΔF, the central frequency of the first one is $+\delta f$ ($\delta f > \Delta F/2$), that of the second one is $-\delta f$. This basic segment is repeated N times, increasing $v_1^{max}{}_{(i)}$ (Maximum amplitudes of selective pulses) and decreasing g_i at each step. A non-selective hard pulse is then applied after the gradient recovery delay τ. For adjustments (b) the excitation pulse is followed by a spin echo with gradients pulses g_r in order to observe the Z-gradient profile of the sample (see Fig. 2).

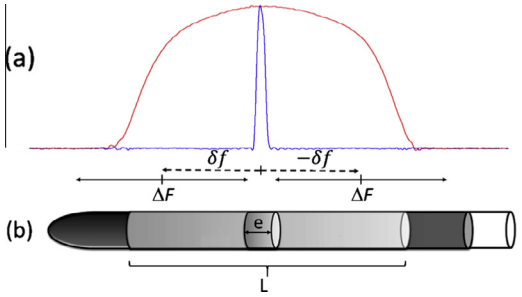

Fig. 2. (a) Phased Z-gradient profiles of an ethanol sample in D_2O (50/50): without (in red) and with (in blue) saturation by Gaussian-OIA pulses [20] of 10 ms with ΔF = 30 kHz, δf = 16 kHz and g_e = 3 G cm^{-1}. (b) Schematic representation of L, height of the sample inside the coil, and e, thickness of the slice detected after saturation by the selective RF pulses. (For interpretation of the references to colour in this figure legend, the reader is referred to the web version of this article.)

of magnetization outside of the central region and obtain the result presented in Fig. 2.

For acquisition of a high resolution spectrum without radiation damping, the sequence is terminated by a hard pulse (Fig. 1a). For adjustments of the selective pulse power and the number of basic segments the excitation pulse is followed by a spin echo with gradients pulses g_r in order to observe the Z-gradient profile of the sample (Fig. 1b).

Radiation damping is therefore controlled by reducing the spatial area and as a consequence the number of spins contributing to the signal detected by the receiver. All the longitudinal magnetization is eliminated and only transverse magnetization from a slice of thickness e is detected, with:

$$e = \frac{2 \cdot \delta f - \Delta F}{\gamma \cdot g_e} \tag{1}$$

The delay between the end of last gradient pulse and the signal sampling are governed by T_1 and not by T_2. Accordingly, the thickness of the slice e can therefore be freely chosen by adjusting δf.

2.2. Optimization

Frequency-swept RF pulses were used for saturation because such pulses reduced the peak B_1 requirements compared with amplitude-only modulated pulses of the same bandwidth. Furthermore, the transverse magnetization generated by frequency-swept RF pulses has a quadratic phase frequency relationship, which is advantageous for dephasing [19].

Duration and shape of the frequency-swept RF pulses determine both the sharpness of turnoff at the edge of saturation region and level of energy deposition. Different shapes and duration were evaluated. As the best compromise we found: Gaussian amplitude modulation, offset independent adiabaticity [20], 10 ms of pulse duration and a 30 kHz frequency sweep.

The minimum value of N needed to obtain a complete saturation of the outer volume magnetization depends on the level of RF inhomogeneity of the coil used. In our case, N = 6 allowed a complete saturation of the outer volume.

Maximum amplitudes of selective pulses ($v_1^{max}{}_{(i)}$) must be increased from one basic segment to the following. We found that good results were obtained using a geometrical progression:

$$v_1^{max}{}_{(i+1)} = \varepsilon \cdot v_1^{max}{}_{(i)}. \tag{2}$$

$v_1^{max}{}_{(1)}$ was adjusted to obtain a good signal suppression in the central part of the profile with the sequence presented in Fig. 1b and with N = 1; $v_1^{max}{}_{(N)}$ was adjusted to obtain a good signal suppression on the edge of the profile, and ε was chosen to satisfy: $v_1^{max}{}_{(N)} = \varepsilon^{(N-1)} . v_1^{max}{}_{(1)}$.

As mentioned in the previous part, it is also essential to reduce g_i at each step in order to avoid spurious echoes during the saturation train. In this way the strongest gradient pulse was placed just after the selective pulse which generates the largest amount of transverse magnetization. Additionally the interval between the strongest gradient and the sampling period is maximum, which minimize the impact of Eddy currents [18]. In practice, we used $g_1 = 40$ G cm^{-1} (80% of g^{max}, the maximum gradient strength on our system) and:

$$g_{i+1} = g_i/1.515 \tag{3}$$

in order to obtain $g_6 = 5$ G cm^{-1} (10% of g^{max}).

The gradient recovery delay τ was optimized by increasing it up to the value for which the peak shape distortion due to Eddy currents are suppressed.

3. Results and discussion

3.1. Suppression of radiation damping

In order to demonstrate the suppression of radiation damping, ^{1}H NMR acquisitions were performed on a solution of ethanol in D_2O (50/50). The methyl triplet of ethanol is displayed in Fig. 3 for three spectra. The first one was obtained using a one pulse acquisition with a small flip angle (9°) and after careful tuning of the coil. Such a small angle avoids any saturation of the receiver but did not suppress the radiation damping effect on peak shapes. This is attested by relative phases dephasing and intensity distortion between lines of the multiplet (Fig. 3a). The same acquisition performed after detuning of the coil restores a regular shape for the multiplet as it is shown in Fig. 3c. An acquisition with the DWET sequence on the same sample and without detuning provided the same result with the same phase shift between the B_1 field and the flipped magnetization (Fig. 3b) demonstrating that Radiation Damping was eliminated although the flip angle was here $\pi/2$ [21,22]. A reduction of the line width was also observed in Fig. 3b, in agreement with the reduced size of the detected volume (better B_0 homogeneity). It must be noted that no line shape distortion due to Eddy currents effect were observed in Fig. 3b.

3.2. Quantitative measurements

In order to evaluate the accuracy of quantitative measurements performed with the DWET sequence, ^{1}H NMR acquisitions were performed on a model preparation of cyclooctane and decamethylcyclopentasiloxane (DMCPS). These two compounds were purchased with a certificate of analysis attesting their purities. They are liquid at room temperature, not hygroscopic, have a low volatility and are miscible. All these features guarantee good preparation conditions and an accurate determination of the concentration ratio by gravimetric method.

Two mixtures were prepared with DMPCS and cyclooctane in acetone-d_6. For each preparation, five consecutive spectra were collected. For both preparations, the concentration ratio was determined from mass and purity using Eq. (1):

$$K' = \frac{m^{DM} \cdot P^{DM} \cdot M^{CO}}{m^{CO} \cdot P^{CO} \cdot M^{DM}} \tag{4}$$

With: m = mass used, P = mass Purity grade, superscript DM indicating DMPCS parameter and superscript CO indicating cyclooctane parameter.

For each spectrum, the concentration ratio was also determined from DWET spectra using Eq. (5):

$$K = \frac{S^{DM} \cdot n_H^{CO}}{S^{CO} \cdot n_H^{DM}} \tag{5}$$

With: S = proton signal area of the quantified site, n_H = number of equivalent hydrogen associated to the quantified site.

Then the trueness of the concentration ratio determination was calculated using the parameter:

$$\Delta = 1000 \cdot \frac{K' - K}{K'} \tag{6}$$

The precision was obtained using relative standard deviation (RSD) calculated from five consecutive spectra.

Results of these measurements and calculations are given in Table 1 (note that these two parameters are expressed in per mille and not in percent).

A very high precision was reached with the DWET sequence as shown in Table 1. The repeatability, obtained by the RSD value, was lower than 1‰ (i.e., 0.1%) for the two preparations. As for Δ, the relative shift of K from the value obtained by gravimetric method (K'); it is lower than 0.65‰ (i.e., 0.065%). These values fulfill the criterion for all quantitative measurements presently performed using ^{1}H NMR.

One potential drawback of the proposed method is the duration of the saturation part, about 26 ms per basic segment. If T_1 of the measured lines is too short, a significant recovery between segments can be induced, which decreases the saturation efficiency. In order to evaluate this point, two other cyclooctane-DMCPS mixtures were prepared with reduced T_1 (by adding a relaxation agent: $Cr(Acac)_3$).

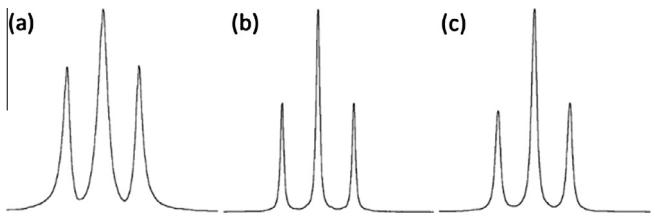

Fig. 3. Methyl region of ^{1}H NMR spectra obtained on a solution of ethanol in D_2O (50/50) at 400 MHz with : (a) single excitation with 9° flip angle, (b) DWET pulse sequence and (c) single excitation with 9° flip angle after coil detuning.

Table 1
Trueness (Δ) and precision (RSD) of the concentration ratio determination using the DWET sequence.

Preparation	1	2
K[a]	0.24	0.30
RSD (‰)[b]	0.73	0.13
Δ (‰)[c]	0.31	0.65

[a] Average value calculated from five consecutive spectra.
[b] Precision (Relative standard deviation calculated from five consecutive spectra).
[c] Trueness from Eq. (6): $(1000(K - K')/K)$.

Table 2
Trueness (Δ) and precision (RSD) of the concentration ratio determination using the DWET sequence on mixture with different T_1 values.

$[Cr(Acac)_3]$	6.25 mM[d]	12.5 mM[e]
K[a]	0.31	0.30
RSD (‰)[b]	0.33	0.44
Δ (‰)[c]	1.79	9.07

[a] Average value calculated from five consecutive spectra.
[b] Precision (relative standard deviation calculated from five consecutive spectra).
[c] Accuracy $(1000(K - K')/K)$.
[d] $T_1^{DMCPS} = 0.41$ s and $T_1^{CO} = 0.39$ s.
[e] $T_1^{DMCPS} = 0.32$ s and $T_1^{CO} = 0.35$ s.

Results of these measurements and calculations are given in Table 2.

Very good repeatability (RSD) was observed for these two preparations. For the mixture with a $Cr(Acac)_3$ concentration of 6.25 mM, the two T_1 were close to 0.4 s and the bias (shift in trueness) is increased up to only 1.79‰ (about 0.2%) which is good enough for most quantitative NMR applications. However, in the case of the mixture with a $Cr(Acac)_3$ concentration of 12.5 mM, for which the two T_1 are 0.32 s and 0.35 s, the bias reached 9‰ (about 1%) and so changed by one order of magnitude.

The protocol presented here therefore seems very efficient for T_1 larger than 0.5 s. For smallest T_1, trueness was slightly reduced but remained on the order of a few percent which is still sufficient for most quantitative applications. T_1 smaller than 0.3 s have not been evaluated in this study but it can be anticipated that the DWET method (in the version presented here) will be in this case less accurate.

4. Conclusion

The DWET sequence allows an efficient radiation damping suppression in ^1H NMR spectra obtained in the context of concentrated samples. The size of the detected volume can be easily chosen in a large range as well as line shape distortions are avoided thanks to uniform signal suppression, including the edge of the coil's volume where the RF efficiency is very poor. Very accurate measurement can be therefore performed. This sequence could be easily incorporated in multi-pulse experiments (including 2D acquisitions).

Some improvements can be considered in order to reduce the duration of the saturation pulse train. Asymmetric RF pulse shapes could be used in order to obtain an increased efficiency on the edge of the sensitive volume, which could consequently reduce the demand on the number of basic segments. Another way could be the simultaneous excitation of the two saturated regions by cosine modulation of the RF profiles, which will divide by two the number of selective pulses. These two strategies are currently under investigation.

5. Experimental

The chemicals were purchased as the following: Absolute ethanol ($P > 99.8\%$) was purchased from VWR Prolabo, cyclooctane from Fluka ($P > 99.5\%$), decamethylcyclopentasiloxane (DMCPS) from Tokyo Chemical Industry ($P > 99.5\%$), Tris(2,4-pentadionato) chromium(III) [$Cr(Acac)_3$] was from Merck. Acetone-d_6 was obtained from Eurisotop.

The ethanol sample was prepared by dissolving it in D_2O (50% v/v). Samples used for quantitative measurements were all prepared by determining carefully masses of both cyclooctane (45 mg) and decamethylcyclopentasiloxane (DMCPS, 190 mg) with the help of a precision balance (Mettler Toledo; d = 1 μg). 600 μL of acetone-d_6 was later added to the preparation.

For T_1 shortening, $Cr(Acac)_3$ solution was prepared as follows: in a vial of 4 mL, 8.7 mg of $Cr(Acac)_3$ were dissolved in 250 μL of acetone-d_6 obtain a 0.1 M concentration. Samples corresponding to concentrations of 6.25 and 12.5 mM were prepared by weighing carefully cyclooctane and DMCPS, then adding 50 and 100 μL of the previously prepared 0.1 M $Cr(Acac)_3$ solution to which were added respectively 550 and 500 μL of acetone-d_6 before being added to the samples. The resulting preparations were thoroughly mixed to ensure complete homogenization and then transferred to an NMR tube using a Hamilton glass syringe without filtration in order to avoid sample loss.

K' ratio was then calculated using Eq. (4).

All the NMR spectra were recorded at 303 K, with no tube rotation, on a Bruker Avance I 400 spectrometer, at a frequency of 400.13 MHz with a 5 mm o.d. dual $^1H/^{13}C$ probe including z-axis gradients. Power of hard pulse was adjusted to obtain $\pi/2$ pulse of 10 μs in duration for ^1H. The repetition delay between each 90° pulse was set at $10 \times T_1^{max}$ of the molecules under investigation to ensure full relaxation of the magnetization. Each measurement was made from five independent NMR recordings.

The selective pulses were performed using 10 ms frequency-swept RF pulse with Gaussian amplitude modulation of the RF field, offset independent adiabaticity and a 30 kHz frequency sweep. The basic segment is repeated 6 times, increasing ν_1^{max} using equation 2 (with $\varepsilon = 1.25$) and reducing g_i using Equation (3) at each step as described in the "Method" section. (Typically, $\nu_1^{max} = 2.9$ kHz corresponds to a $\pi/2$ flip angle in the middle of the sample and $g_1 = 40$ G cm^{-1}). The duration of spoiling gradient g_i was 3 ms and each of them was followed by a 1 ms recovery delay. An additional gradient recovery delay τ of 1 ms was added before the $\pi/2$ hard pulse. The g_e and g_r gradients were applied with the following strengths: 3 G cm^{-1} and 2.5 G cm^{-1}.

FIDs were processed with: an exponential multiplication inducing a line broadening of 1.7 Hz, zero-filling to 128 K before Fourier transform, manual phasing and automatic baseline correction, using a polynomial function (order 1). The spectra were processed in the frequency domain; peak areas were determined by the curve-fitting process implemented within Perch Software (Perch NMR software™, Perch Solutions Ltd, Kuopio, Finland).

Acknowledgments

K. Bayle thanks the French Research Ministry for financial support and we thank the CNRS and University of Nantes for financial support through core funding.

References

[1] U. Holzgrabe, Quantitative NMR spectroscopy in pharmaceutical applications, Prog. Nucl. Mag. Reson. Spec. 57 (2010) 229–240.
[2] J.C. Lindon, J.K. Nicholson, E. Holmes, J.R. Everett, Metabonomics: metabolic processes studied by NMR spectroscopy of biofluids, Conc. Mag. Reson. 12 (2000) 289–320.
[3] S. Zhang, G.A. Nagana Gowda, V. Asiago, N. Shanaiah, C. Barbas, D. Raftery, Correlative and quantitative ^1H NMR-based metabolomics reveals specific metabolic pathway disturbances in diabetic rats, Anal. Biochem. 383 (2008) 76–84.
[4] G.F. Pauli, QNMR – a versatile concept for the validation of natural product reference compounds, Phyto. Anal. 12 (2001) 28–42.
[5] A. Menditto, M. Patriarca, B. Magnusson, Understanding the meaning of accuracy, trueness and precision, Accred. Qual. Assur. 12 (2007) 45–47.
[6] G. Suryan, Nuclear magnetic resonance and the effect of the methods of observation, Cur. Sci. 6 (1949) 203–204.
[7] N.V. Bloembergen, R.V. Pound, Radiation damping in magnetic resonance experiments, Phys. Rev. 95 (1954) 8–13.
[8] V.V. Krishnan, N. Murali, Radiation damping in modern NMR experiments: progress and challenges, Prog. Nucl. Mag. Res. Spectr. 68 (2013) 41–57.
[9] P. Broekaert, J. Jeener, Suppression of radiation damping in NMR in liquids by active electronic feedback, J. Mag. Reson. Ser. A 113 (1995) 60–64.
[10] R. Chidambaram, A method of reducing radiation damping in nuclear magnetic resonance, Nuo. Cim. 13 (1959) 405–409.
[11] C. Anklin, M. Rindlisbacher, G. Otting, F.H. Laukien, A probehead with switchable quality factor – suppression of radiation damping, J. Mag. Reson. Ser. B 106 (1995) 199–201.
[12] W.E. Maas, F.H. Laukien, D.G. Cory, Suppression of radiation damping by q-switching during acquisition, J. Mag. Reson. Ser. A 113 (1995) 274–277.
[13] J.H. Chen, B. Cutting, G. Bodenhausen, Measurement of radiation damping rate constants in nuclear magnetic resonance by inversion recovery and automated compensation of selective pulses, J. Chem. Phys. 112 (2000) 6511–6514.
[14] B. Cutting, J.H. Chen, D. Moskau, G. Bodenhausen, Radiation damping compensation of selective pulses in water-protein exchange spectroscopy, J. Biomol. NMR 17 (2000) 323–330.
[15] C.A. Michal, Defeating radiation damping and magnetic field inhomogeneity with spatially encoded noise, Chem. Phys. Chem. 11 (2010) 3447–3455.
[16] A.K. Khitrin, A. Jerschow, Simple suppression of radiation damping, J. Mag. Reson. 225 (2012) 14–16.

[17] R.J. Ogg, R.B. Kingsley, J.S. Taylor, WET, a T_1- and B_1-linsensitive water-suppression method for in vivo localized ^{1}H NMR spectroscopy, J. Mag. Reson. B 104 (1994) 1–10.
[18] S.H. Smallcombe, S.L. Patt, P.A. Keifer, WET solvent suppression and its applications to LC NMR and high-Rresolution NMR spectroscopy, J. Mag. Reson. A 117 (1995) 295–303.
[19] Y. Luo, R.A. de Graaf, L. DelaBarre, A. Tannus, M. Garwood, BISTRO: An outer-volume suppression method that tolerates RF field inhomogeneity, Mag. Reson. Med. 45 (2001) 1095–1102.
[20] A. Tannus, M. Garwood, Improved performance of frequency-swept pulses using offset-independent adiabaticity, J. Mag. Reson. A 120 (1996) 133–137.
[21] H. Barjat, G.P. Chadwick, G.A. Morris, A.G. Swanson, The behavior of multiplet signals under "radiation damping" conditions. I. Classical effects, J. Mag. Reson. A 117 (1995) 109–112.
[22] D. Shishmarev, G. Otting, Radiation damping on cryoprobes, J. Mag. Reson. 213 (2011) 76–81.